
An Innovative Approach to Measuring Spring Constants: Utilizing 3D Printing and Sound Sensing with Improved Time Resolution in Data Collection

Kalpajit Roy, Sakshi Garg, Ankush Rana,
Shivam Tomar and Amit Garg

Acharya Narendra Dev College, University of Delhi, Delhi,
India

E-mail: amitgarg@andc.du.ac.in

(Submitted 30-04-2023)

Abstract

We have carried out spring constant measurements for a single spring, series, parallel, and parallel series spring combination through sound sensing using a microphone of a simple smartphone. Using a 3D printed rod and open-source Windows-based software called 'Audacity', primarily a sound recording and editing software with a least count of 10 microseconds, has drastically improved the accuracy of spring constant measurements. The results obtained are much more accurate than many that have been previously reported. It has also been concluded that sound-based measurements are more exact than magnetic field-based measurements. Using simple devices with no additional software requirements at the time of experimentation makes it a promising proposition for students with humble background. It will encourage them to take their first step towards technological innovation-based learning.

Keywords: spring constant, sound sensing, 3D printing, smartphone, STEM education

1. Introduction

Spring constant measurement is an omnipresent experiment at secondary and tertiary level education in India. The experiment is performed using both static and dynamic methods in conventional mode [1][2]. With the introduction of the National Education Policy in India in 2020 [3], the students are provided with an opportunity to perform experiments in different innovative ways, including the use of various types of sensors and interfaces. Spring constant measurements have been an area of interest for science educators for a

long time. Kuhn et al. [4] analyzed the spring pendulum phenomenon using the acceleration sensor of a smartphone. Sans et al. [5] used a smartphone's ambient light sensor to understand the oscillatory motion of a two-spring coupled system. Pili et al. [6] measured the spring constant using the smartphone's ambient light sensor with reasonable accuracy. Pili et al. [7] have performed the spring constant measurements using the magnetic field sensor of a smartphone with fair accuracy. Pili et al. have further introduced spring force constant measurement innovation using a magnetic spring-mass oscillator and a telephone pickup [8], an

optical spring-mass system and a solar panel [9], and sound, door alarm, and soundcard oscilloscope [10]. Coban et al. [11] measured the spring constant using an ultrasonic distance sensor and Arduino with an error of 3.45% in a series configuration and 1.13% in a parallel configuration. In a recent work by Listiaji et al. [12], they carried out free and damped oscillation experiments with reasonable accuracy using acceleration and video trackers available on smartphones. In the present studies, we have performed spring constant measurements of three springs of the same type, their series, parallel, and parallel series combination, using a microphone and tone generator of a smartphone. The spring interconnects were made using 3D printing. The results obtained show higher accuracy in comparison to studies reported so far. Some of the key features of the present studies are listed as under:

1. We have used an open-source Windows software called 'Audacity,' primarily a sound recording and editing software. For the first time to the best of our knowledge, it has been used in experimental scientific research. It shows the amplitude of sound recorded with time with a least count of 10 microseconds. One can find the time period between two amplitude maxima through the waveform generated.
2. The standard deviation in the value of the spring constant of a single spring in the case of the audio sensor is lower than that in the case of the magnetic sensor. It depicts that a sound sensor is more precise than a magnetometer. For a complex system of parallel series setup, the accuracy and precision is much higher in case of sound sensing.
3. The percentage error in the case of parallel configuration decreased to 0.59% when a 3D-printed rod with hooks was used instead of a metal rod.
4. The percentage error in the case of parallel series configuration decreased to 0.48%

when a 3D-printed rod with hooks was used instead of a metal rod.

5. Even using Arduino distance sensors, Coban et al. observed an error of 3.45% in a series configuration and 1.13% in a parallel configuration. The errors are higher in comparison to our results.
6. Besides accuracy, sound-based measurements require items readily available in everyone's daily life, like mobile phones and earphones/microphones. The other reported methods need a decent smartphone with decent inbuilt sensors. However, this method works fine even for low-budget phones and microphones.
7. There is no need for data analysis software.
8. There is no impact of ambient noise during the measurements, unlike in magnetic sensor-based experiments where surrounding magnetic objects can disturb the readings.

2. Theoretical Background

2.1 Spring Constant

The spring constant of a spring is a measure of its stiffness, i.e., it helps us calculate how much force (F) is required to produce a set amount of extension (x) in the spring. Mathematically, this is represented by Hooke's law:

$$F = -kx \quad (1)$$

The proportionality constant k is the spring constant.

2.2 Combinations

Springs of different stiffness can even be connected to get a combined effect. In the case of two springs, there are two types of setups for connecting the springs – series setup and parallel setup.

In a series setup (also called double pendulum), one end of the first spring is connected to a rigid support, the second is connected to the upper end of second spring. The lower end of the second spring is connected to the load. If k_1 and k_2 are the spring constants of first and second spring, then the resultant spring constant is given by:

$$\frac{1}{k} = \frac{1}{k_1} + \frac{1}{k_2} \quad (2)$$

For the parallel setup (also called coupled pendulum), upper end of both springs is connected to a rigid support, and the lower end is connected to a common load. Here, the resultant spring constant is given by:

$$k = k_1 + k_2 \quad (3)$$

Also, these combinations can be further permuted to get more complex spring systems. For example, a third spring can be connected in series to a two-spring parallel setup (also called coupled double pendulum), and thus the resultant spring constant becomes:

$$\frac{1}{k} = \frac{1}{k_1 + k_2} + \frac{1}{k_3} \quad (4)$$

2.3 Calculating Time Period

The motion executed by a spring-mass oscillator is one of the most common examples of a simple harmonic motion (SHM), and its time period is calculated using the formula:

$$T = 2\pi \sqrt{\frac{M + m_{eff}}{k}} \quad (5)$$

Where M is the sum of the mass of load and m_{eff} the effective mass of the spring (1/3rd the mass of spring for an ideal spring [13]) and k is the spring constant.

By squaring both sides of equation 5 and rearranging, we get

$$k = \frac{4\pi^2}{T^2} (M + m_{eff}) \quad (6)$$

2.4 Sound-based measurements

Let us take a sound-producing source and a receiver. The intensity of sound obtained increases with the decrease in distance between the source and the receiver. If the receiver executes a simple harmonic motion with respect to the source, and the amplitude is plotted against time, then we get a sinusoidal wave. The time difference between any two consecutive peaks gives the time period of the receiver's motion.

2.5 3D Printing

3D Printing, also known as additive manufacturing, uses a digitally designed 3D model file to create a three-dimensional object layer-by-layer. Here we have used FDM (Fused Deposition Model) technology in which the physical objects are printed by building up successive layers of the material. The metal and 3D printed rods are shown in Fig 1.a and 1.b.



Figure 1.a: Metal rod



Figure 1.b: 3D printed rod

3. Experimental Setup

We used a spring oscillation apparatus that holds the spring's upper end firmly so that the oscillations are stable. A hook carrying the weights is connected to the lower end of the spring. The microphone of an earphone is attached underneath the weights.

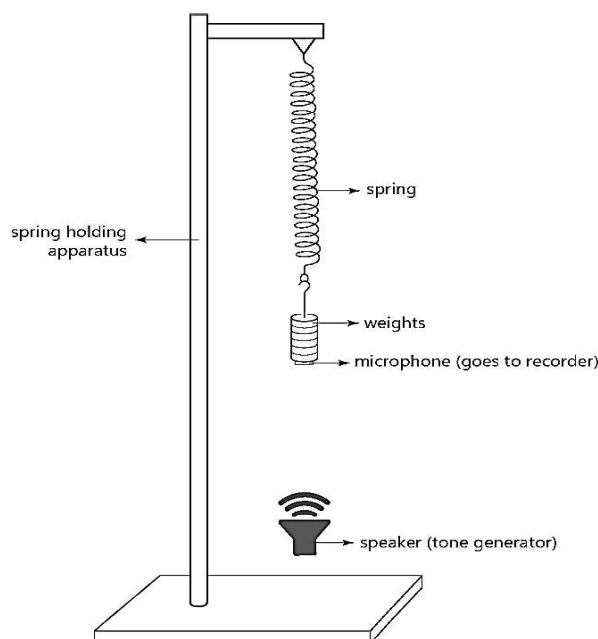


Figure 2: Schematic diagram of experimental setup

A smartphone is kept vertically below the microphone. A constant tone of 900 Hz is generated using the Android application, 'Phyphox'. The spring system is allowed to oscillate vertically by

stretching the spring for a small displacement. The audio received by the microphone is recorded in the recording device. The experimental setup is shown in Fig. 2.

Initially, we used a smartphone with 'Phyphox' application to record and generate a CSV file of sound pressure versus time readings. The file was later opened using MS Excel and the time periods at maximum sound pressure were noted using a graph. We observed that the least count of time was 0.2 seconds, which is too high to get accurate timing of maximum sound pressure.

We switched to the use of a popular audio recording and editing Windows software called 'Audacity'. It solved the issue as the least count of time surpassed the resolution in comparison to the previous value by a huge margin. The recorded audio in Audacity can be visualized as a waveform with amplitude of audio along the vertical axis and time along the horizontal axis. The audio was amplified using the 'Amplify' in-built effect. The timing at maximum amplitude was measured by carefully analyzing the waveform. Weights were varied and readings were taken for different settings. Finally, the spring constant was calculated for all the different weights using the slope of the graph between time-period squared in y-axis and total mass in x-axis. Similarly, the spring constants of spring 2 and spring 3 were also measured. The mass of each weight is measured using a high precision electronic digital balance model PBG 200 with a readability and repeatability of 1 mg. The maximum percentage errors for series, parallel and parallel series combination were calculated using the formula applicable for such combined complex systems. For calculating the error margins theoretically, we used basic error addition, multiplication and division rules for series, parallel and parallel-series systems. In case of addition or subtraction of two uncertainty values, the uncertainty in the value is simply added together. In case of multiplication and division, the percentage errors are directly added. To deal with

complex systems, these rules are applied in combination.

3.1 Series Configuration (Double Pendulum)

Spring 1 was attached to the holder and spring 2 was attached to the lower end of the first spring. The weights were hung on the lower end of the second spring. The system oscillated and audio was recorded and measurement of the spring constant was done. The process was repeated by varying the weights.

3.2 Parallel Configuration (Coupled Pendulum)

We used two spring holder apparatuses to attach spring 1 to one and spring 3 to the other. The lower ends of both springs were connected through a metal rod and the spring constant was measured by oscillating the system as we did in previous cases.

3.3 Parallel-series Configuration (Coupled Double Pendulum)

Now instead of the weights, spring 2 was attached to the center of mass of the rod. The weights were hung on the lower end of spring 2. As usual, we oscillated the system and measured the spring constant using Audacity. The oscillations were unstable with twisting and horizontal movements because of which a higher error is observed in calculated spring constants.

We repeated the experiment with a 3D-printed rod with hooks to connect the springs or weights. We designed a 3D Printed rod of 10.495 gm weight, where PLA (Polylactic Acid) was used as a filament with 100% infill density. We used a free online 3D modeling software called 'TinkerCAD' to design the prototype model of the Rod. 'Flashforge Creator 3 Pro' was used to print the Rod model.

To scale the model and precisely measure the distance between the two neighboring hooks, which place the rod's center of mass at the lower central hook, we used 'FlashPrint' software. The oscillations were remarkably more stable now and we recorded better results.

The experimental setups are as shown in Fig 3.a to 3.d.

3.4 Parallel configuration with 3D printed rod

After the success with the parallel series configuration, we repeated the experiment with just parallel configuration by using the 3D printed rod instead of the metal rod. We could observe a more accurate value.



Figure 3: Experimental setup for: a. single spring, b. series configuration, c. parallel configuration, d. parallel-series configuration

3.5 Sound vs. Magnetic field-based sensing

For comparison of our technique with other smartphone sensor-based techniques, we calculated the spring constant of spring 1 using the magnetometer in a smartphone. A magnet was attached to the weight hanger. A smartphone was kept vertically below the magnet at a distance. As the spring oscillated, the magnetic field around the smartphone changed and the value was recorded using the android application, 'Physics Toolbox Sensor Suite'. The time period between successive maximum magnetic fields was noted from the CSV file and the value of the spring constant was found using equation 6. We also measured the spring constant in the case of parallel-series configuration using this technique.

4. Results

4.1 Single Spring 1

We observed very good accuracy in spring constant values for the five different weights for the first single spring after sound sensing calculations. We discovered that the heaviest weight had a bit of high deviation, most likely due to damping. We discovered that the standard deviation of the spring constants is **0.0645**. The percentage error is **0.91%**.

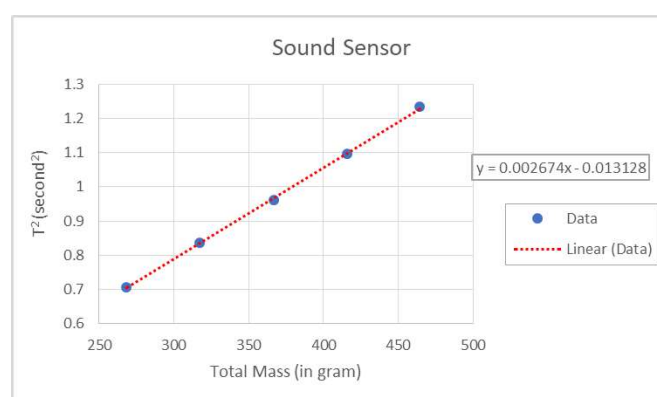


Figure 4: Graph for single spring using sound sensing

The spring constant's mean value was calculated to be **14.764 N/m**. The slope of the T^2 vs total mass graph is a straight line as shown in Fig 4.

For the same five different weights, we discovered that magnetic sensing had lower precision than sound sensing. The heaviest weight also displayed similar high deviation. The measured spring constant has a standard deviation of **0.1529**. The spring constant's mean value was calculated to be **15.2065 N/m**. The T^2 vs total mass graph shows deviation from a precise straight line as shown in Fig 5:

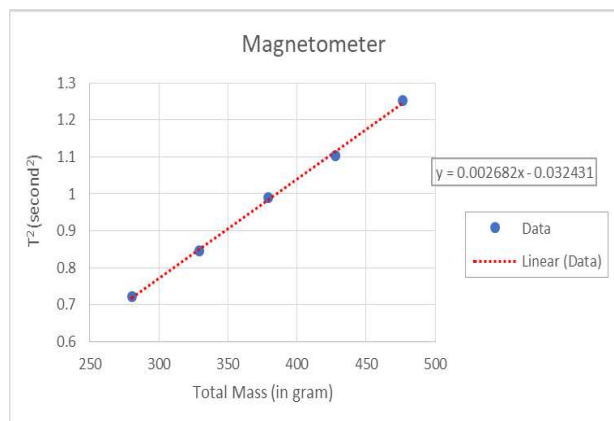


Figure 5: Graph for single spring using magnetometer

It is clearly seen from Fig 4 and Fig 5, the linear fit using the sound-based measurements is much better than magnetic based measurements. The percentage error between sound based and magnetic based measurements is **1.215%**.

4.2 Single Spring 2

The sound-based measurements were repeated as described in section 4.1 for spring 2. The spring constant's mean value was calculated to be **14.841 N/m** with **0.0513** as the standard deviation. The percentage error is **0.32%**

4.3 Single Spring 3

The sound-based measurements were repeated as described in section 4.1 for spring 3. The spring constant's mean value was calculated to be **15.103 N/m** with **0.0525** as the standard deviation. The percentage error is **1.36%**

4.4 Series Configuration

The sound-based measurements were repeated as described in section 3.1. The measured mean value

of the spring constant is **7.580 N/m** as calculated from the graph as shown in Fig 6. The standard deviation equals **0.0465**. The calculated series connection value is **7.401 N/m** and the percentage error is approximately **2.42%**.

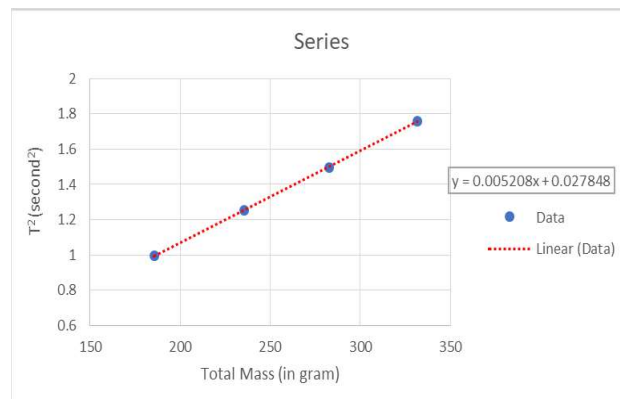


Figure 6: Graph for series configuration using sound sensing

4.5 Parallel Configuration

The sound-based measurements were repeated as described in section 3.2. When we used a **metal rod** for the parallel spring system. The spring constant's mean value was determined to be **29.506 N/m** from the graph as shown in Fig 7 with **0.1257** as the standard deviation. The calculated parallel connection value is **29.866 N/m**. The percentage error is around **1.21%**.

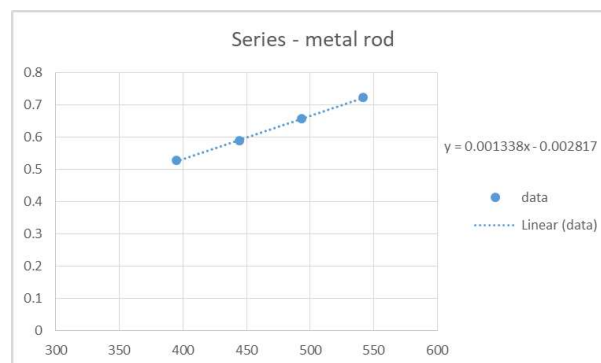


Figure 7: Graph for parallel configuration using sound sensing (with metal rod)

When we repeated the same experiment with the **3D-printed rod**. The mean value of the spring constant was found to be **30.044 N/m** from the graph as shown in Fig 8. with standard deviation as **0.0805**. The calculated value of the parallel

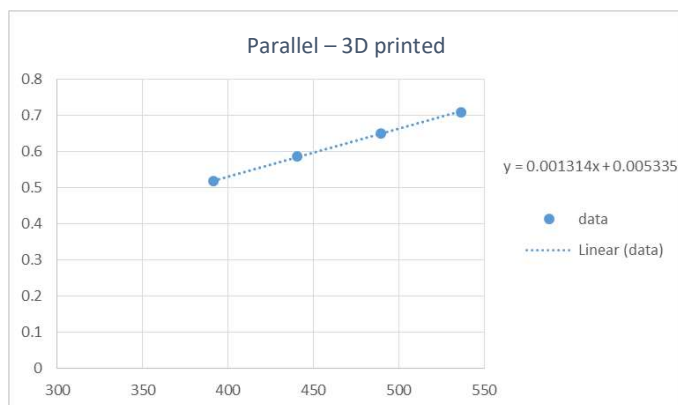


Figure 8: Graph for parallel configuration using sound sensing (with 3D-printed rod)

connection is **29.866 N/m**. The percentage error is around **0.59%**.

4.6 Parallel series Configuration

The sound-based measurements were repeated as described in section 3.3. We used a **metal rod** to perform the experiment for the parallel-series spring system. The mean value of the spring constant was determined to be **9.813 N/m** with **0.4562** as the standard deviation. The calculated parallel series connection value is **9.915 N/m**. The percentage error was approximately **1.02%**.

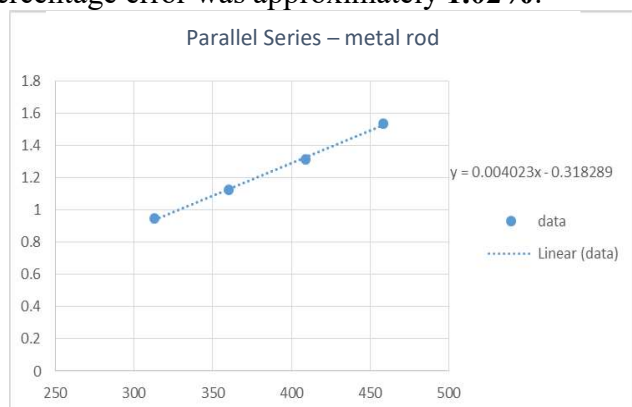


Figure 9: Graph for parallel-series configuration using sound sensing (with metal rod)

We repeated the same experiment for the parallel-series system of springs with the **3D-printed rod**. The spring constant's mean value was determined to be **9.867 N/m** from the graph as shown in Fig 10 with **0.1953** as the standard deviation. The calculated parallel series connection value is **9.915 N/m**. The percentage error was approximately **0.48%**.

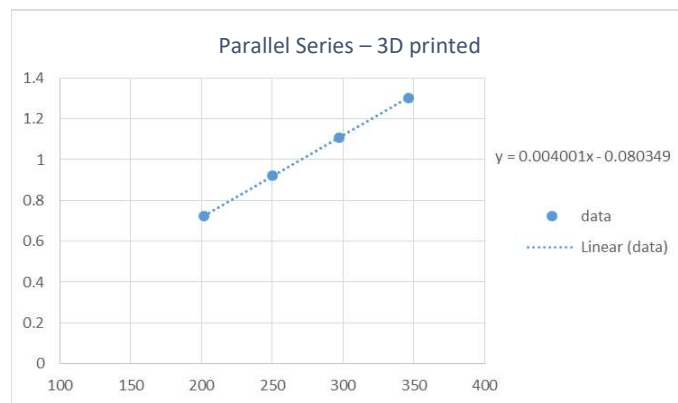


Figure 10: Graph for parallel-series configuration using sound sensing (with 3D-printed rod)

4.7 Comparison with Magnetic field measurement

In order to ascertain the accuracy based on sound and magnetic field measurements, we took observations of a parallel series configuration with magnetic field measurements using the **3D-printed rod**. The spring constant's mean value using magnetic field measurements was determined to be **16.679 N/m**. The calculated parallel series connection value is **9.915 N/m**. The standard deviation is approximately **0.451**. The percentage error is approximately **21.83%**.

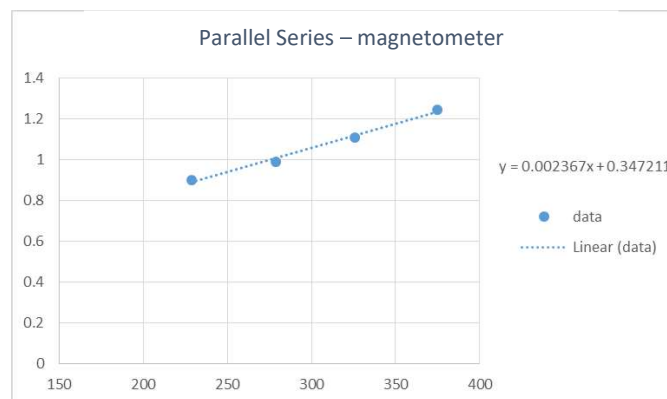


Figure 10: Graph for parallel-series configuration using magnetometer (with 3D-printed rod)

4.8 Calculation of Theoretical Error:

To calculate absolute error in the theoretical values of each of the three combinations, two fundamental rules are followed:

1. When adding or subtracting two values, their absolute errors are always added.

2. When multiplying or dividing two values, their percentage errors are added directly.

The absolute errors can be calculated from the percentage errors for each individual spring.

For series combination:

$$k_s = \frac{k_1 k_2}{k_1 + k_2} = \frac{14.764 \times 14.841}{14.764 + 14.841} \pm \frac{(0.91 + 0.39)\%}{0.13 + 0.06}$$

$$= \frac{219.11}{29.605} \pm \frac{1.3\%}{0.64\%} = 7.401 \pm 1.94\% = 7.401 \pm 0.02 \text{ N/m}$$

For parallel combination:

$$k_p = k_1 + k_2 = 14.764 + 15.103 \pm 0.13 + 0.2 = 29.867 \pm 0.33 \text{ N/m}$$

For parallel series combination:

$$k_{ps} = \frac{(k_1 + k_3)k_2}{k_1 + k_2 + k_3} = \frac{443.25}{44.708} \pm \frac{(1.09 + 0.39)\%}{0.5} = \frac{443.25}{44.708} \pm \frac{1.48\%}{1.11\%} = 9.915 \pm 0.03 \text{ N/m}$$

All the results in section 4 have been summarized in the following table (Table 1).

Table 1: Summary of the experimental measurements:

System	Spring Constant (N/m)	Measured Spring Constant (N/m)	Standard Deviation	% Error
Spring 1	$k_1 = 14.9 \pm 0.1^*$	$k_1 = 14.764$	0.0645	0.91%
Spring 2	$k_2 = 14.9 \pm 0.1^*$	$k_2 = 14.841$	0.0513	0.39%
Spring 3	$k_3 = 14.9 \pm 0.1^*$	$k_3 = 15.103$	0.0525	1.36%
Series combination of Spring 1 and Spring 2 $\frac{1}{k} = \frac{1}{k_1} + \frac{1}{k_2}$	$k = 7.401 \pm 0.02$	$k = 7.580$	0.0465	2.42%
Parallel combination of Spring 1 and Spring 3 (Interconnect using Metal Rod) $k = k_1 + k_3$	$k = 29.866 \pm 0.33$	$k = 29.506$	0.1257	1.21%
Parallel combination of Spring 1 and Spring 3 (Interconnect using 3D Printed Rod) $k = k_1 + k_3$	$k = 29.866 \pm 0.33$	$k = 30.044$	0.0805	0.59 %
Parallel combination of Spring 1 and Spring 3 in series with spring 2 (Interconnect using Metal Rod) $\frac{1}{k} = \frac{1}{k_1 + k_3} + \frac{1}{k_2}$	$k = 9.915 \pm 0.03$	$k = 9.813$	0.4562	1.02 %

Parallel combination of Spring 1 and Spring 3 in series with spring 2 (Interconnect using 3D Printed Rod) $\frac{1}{k} = \frac{1}{k_1 + k_3} + \frac{1}{k_2}$	$k = 9.915 \pm 0.03$	$k = 9.867$	0.1953	0.48 %
Using Magnetic Field sensing: Parallel combination of Spring 1 and Spring 3 in series with spring 2 (Interconnect using 3D Printed Rod) $\frac{1}{k} = \frac{1}{k_1 + k_3} + \frac{1}{k_2}$	$k = 9.915 \pm 0.03$	$k = 16.679$	0.451	68.223 %.

* As provided by the supplier

5. Conclusion

In the present experiment, we have demonstrated that the spring constant can be effectively measured using an earphone's microphone. Data can be recorded and analyzed using the 'Audacity' application on a laptop. Most of the earlier papers have used Android applications such as 'Physics Toolbox Sensor Suite' and 'Phyphox' with different sensors to measure time period of oscillations. But, in case of audio sensing, we found that Phyphox has too high least count and Physics Toolbox Sensor Suite had very unstable readings. However, Audacity can show the amplitude of sound recorded with time with a least count of 10 microseconds. Audacity is a software predominantly used for recording and editing and to the best of our knowledge, it is the first time this editing software has been used in such experiments.

The values of spring constant matches with the theoretical values for series and parallel configuration with exceptional accuracy, where the percentage error is as low as 0.48% in case of parallel series which is the most complex system here. The parallel-series system shows comparably higher error with steel rod. The rod used in the parallel-series combination was changed and designed using a 3D printer. It is light-weighted, custom designed and provides much higher

accuracy as compared to the metal rod. Hence, the results came out better than that of the steel rod. We have competitively compared our method with magnetic sensing technique. It turns out that a sound sensor is a bit more precise in simple systems having a single spring, but both showed similar accuracy. But in case of complex systems, such as parallel series setup, the results are broadly more accurate and precise than magnetic field measurements.

Another significant advantage of sound-based measurements is that the ambient noise does not cause any disturbance in readings, unlike as with magnetic field where surrounding objects get magnetized and disrupts the reading. Apart from high accuracy, the simplicity and readily available requirements for the technique has to be noted. It requires items that are easily available in everyone's daily life like mobile phones and earphone/microphone. All the other similar methods to find spring constant require a decent smartphone having decent sensors installed. However, this method will work fine on low-budget phones and microphones at the time of experiment. Thus, its acceptability and motivation for students of all backgrounds will be much higher in India. The recorded audio file can later be analyzed using any computer with Audacity. Furthermore, no separate

data analysis software is needed to find the time period.

Acknowledgement

Authors are thankful to Principal, Acharya Narendra Dev College for providing infrastructural support. The financial support for the equipments under DBT Star College scheme, Department of Biotechnology, is gratefully acknowledged. The financial and the peer group support in the present studies under SPIE Student Chapter, University of Delhi at ANDC is duly acknowledged.

References

- [1] (2023) *Ncert.nic.in*. Available at: <https://ncert.nic.in/pdf/publication/sciencelaboratorymanuals/classXI/physics/kelm105.pdf> (Accessed: 26 February 2023).
- [2] (2023) *Physics.du.ac.in*. Available at: https://physics.du.ac.in/pdfs/BSc_syll/Bsc_hons_phys.pdf (Accessed: 26 February 2023).
- [3] (2023) *Ugc.ac.in*. Available at: https://www.ugc.ac.in/pdfnews/5294663_Salient-Featuresofnep-Eng-merged.pdf (Accessed: 26 February 2023).
- [4] Kuhn, J. and Vogt, P. (2012) "Analyzing spring pendulum phenomena with a smart-phone acceleration sensor", *The Physics Teacher*, 50(8), pp. 504-505. doi: 10.1119/1.4758162.
- [5] Sans, J.A. *et al.* (2013) "Oscillations studied with the smartphone ambient light sensor," *European Journal of Physics*, 34(6), pp. 1349–1354. Available at: <https://doi.org/10.1088/0143-0807/34/6/1349>.
- [6] Pili, U. (2018) "A dynamic-based measurement of a spring constant with a smartphone light sensor," *Physics Education*, 53(3), p. 033002. Available at: <https://doi.org/10.1088/1361-6552/aaa927>.
- [7] Pili, U. and Violanda, R. (2019) "Measuring a spring constant with a smartphone magnetic field sensor," *The Physics Teacher*, 57(3), pp. 198–199. Available at: <https://doi.org/10.1119/1.5092488>.
- [8] Pili, U. and Violanda, R. (2019) "Measuring a spring constant with a magnetic spring-mass oscillator and a telephone pickup," *Physics Education*, 54(4), p. 043001. Available at: <https://doi.org/10.1088/1361-6552/ab1432>.
- [9] Pili, U.B. (2019) "Measuring a spring constant using an optical spring-mass system and a solar panel," *Physics Education*, 55(1), p. 013003. Available at: <https://doi.org/10.1088/1361-6552/ab5399>.
- [10] Pili, U.B. and Violanda, R.R. (2021) "Measurement of a spring force constant using sound, door alarm, and soundcard oscilloscope," *Physics Education*, 56(6), p. 063005. Available at: <https://doi.org/10.1088/1361-6552/ac1c4a>.
- [11] Çoban, A. and Çoban, N. (2020) "Determining of the spring constant using Arduino," *Physics Education*, 55(6), p. 065028. Available at: <https://doi.org/10.1088/1361-6552/abb58b>.
- [12] Listiaji, P. *et al.* (2020) "Comparison between the use of acceleration sensor and video tracker on smartphone for Spring Oscillation Experiment," *Physics Education*, 56(1), p. 013001. Available at: <https://doi.org/10.1088/1361-6552/abb88b>.
- [12] Rodríguez, E.E. and Gesnouin, G.A. (2007) "Effective mass of an Oscillating spring," *The Physics Teacher*, 45(2), pp. 100–103. Available at: <https://doi.org/10.1119/1.2432087>.